JOURNAL OF NEUROPHYSIOLOGY
Vol. 68, No. 4, October 1992. *Printed in U.S.A.*

Simulation of the Currents Involved in Rhythmic Oscillations in Thalamic Relay Neurons

JOHN R. HUGUENARD AND DAVID A. McCORMICK
Department of Neurology and Neurological Sciences, Stanford University Medical Center, Stanford, California 94305-5300; and Section of Neurobiology, Yale University School of Medicine, New Haven, Connecticut 06510

SUMMARY AND CONCLUSIONS

1. To perform simulations of the various modes of action potential generation in thalamic relay neurons, we developed Hodgkin-and-Huxley style mathematical equations that describe the voltage dependence and kinetics of activation and inactivation of four different currents, including the transient, low-voltage-activated Ca^{2+} current (I_T), the rapidly inactivating transient K^+ current (I_A), the slowly inactivating K^+ current (I_{K2}), and the hyperpolarization-activated, mixed cationic current (I_h). The modeled currents were derived either from acutely dissociated rat thalamic relay neurons (I_T, I_A, I_{K2}), or from guinea pig thalamic relay cells maintained in slices in vitro (I_h).

2. The voltage dependence of steady-state activation and inactivation of I_T, I_A, and I_{K2} and the activation of I_h could be modeled with Boltzmann-style equations. Modeling of the behavior of I_T to depolarizing steps in voltage clamp required the use of the constant field equation to relate permeability to T-current amplitude. The time constant of activation of I_T was described by a continuous bell-shaped function with a maximum near 15 ms at threshold for activation (−75 mV) and 23°C. Mathematical description of the kinetics of inactivation and removal of inactivation of this current required two separate functions.

3. The rapidly activating and inactivating K^+ current I_A was modeled by assuming two components with different time constants of inactivation. The kinetics of activation was described as a continuous function of voltage with the slowest time constant, near 2.5 ms, at threshold for activation (−60 mV) and 23°C. In contrast, the kinetics of inactivation of both components were described as voltage independent, consistent with experimental data. The rate or removal of inactivation of both components of I_A was described as continuously increasing with the degree of hyperpolarization.

4. The slowly inactivating K^+ current I_{K2} was also modeled by assuming two components with different rates of inactivation. The kinetics of activation were described by a bell-shaped function with a maximum time constant near 80 ms at −40 mV and 23°C, whereas threshold for activation was approximately −60 mV. Inactivation of both components was modeled as relatively independent of voltage, whereas removal of inactivation was described as a continuous function of membrane potential.

5. The hyperpolarization-activation cationic current, I_h, was modeled by assuming that the current activates with a single exponential relation and does not inactivate. The kinetics of activation and deactivation of I_h were described by a continuous and bell-shaped function of membrane potential, with the slowest rate of activation (time constant of ~1 s at 35°C) occurring at −80 mV, which is near the membrane potential for half activation (−75 mV).

6. The analysis and modeling of the voltage dependence, kinetics, and reversal potentials of these four currents, I_T, I_A, I_{K2}, and I_h, predict that I_T should provide the inward current for the generation of low-threshold Ca^{2+} spikes, with the rapidly activating and inactivating K^+ current I_A modulating the initial components of these Ca^{2+} spikes. In contrast, the slower kinetics of activation and inactivation of the K^+ current I_{K2} suggest that this current may affect more the later portions of low-threshold Ca^{2+} spikes. The properties of I_h suggest that it is critical to modulation of the voltage-time course of the cell at hyperpolarized membrane potentials and may provide a "pacemaker" potential for rhythmic burst generation.

INTRODUCTION

Thalamic relay neurons are capable of firing Na^+-dependent spikes in a variety of patterns (Deschênes et al. 1982; Llinás and Jahnsen 1982), which occur in stereotyped fashion during different states of behavioral arousal (reviewed in Steriade and Deschênes 1984; Steriade and Llinás 1988). The spike firing patterns are, in turn, determined by the array of voltage-dependent ion channels present within the relay neuron plasma membrane. One interesting feature of thalamic relay neurons is their ability to generate rhythmic bursts discharges, owing to the occurrence of low-threshold Ca^{2+} spikes (Jahnsen and Llinás 1984a,b; McCormick and Pape 1990; Steriade et al. 1991). Several currents have been identified that are activated in the range of potentials near the threshold for action potential generation and that are likely to be involved in this generation of rhythmic low-threshold Ca^{2+} spikes. These currents include I_T, the low-threshold, transient Ca^{2+} current that underlies burst firing (Coulter et al. 1989; Crunelli et al. 1989; Hernández-Cruz and Pape 1989; Huguenard and Prince 1992; Suzuki and Rogawski 1989); the rapidly inactivating and transient K^+ current, I_A (Huguenard et al. 1991), which may facilitate slow repetitive firing (Connor and Stevens 1971) and may interact with I_T during Ca^{2+}-dependent burst firing (Huguenard et al. 1991); a slowly inactivating transient K^+ current, I_{K2} (Huguenard and Prince 1991), which may control repetitive firing rate; and a hyperpolarization-activated, mixed cationic conductance with slow kinetics, I_h (McCormick and Pape 1990; Pape and McCormick 1989), which activates on hyperpolarization and which may generate a "pacemaker" potential for the generation of slow oscillations. In this paper we collect both published and unpublished voltage-clamp data and present mathematical descriptions of these four separate ionic conductances. Our

goal was to use the results of these voltage-clamp experiments to obtain the parameters necessary to simulate voltage and current behavior in a model thalamocortical relay neuron. In the following paper (McCormick and Huguenard 1992) we present the results of voltage simulations in which multiple relay neuron firing modes are reproduced.

METHODS

As in the studies of Hodgkin and Huxley (1952), each macroscopic current was modeled as being comprised of a population of equivalent microscopic ion channels. Each channel is controlled by at least one gate, and all gates of any individual channel must be open for the channel to be conducting. The gate opening and closing rates are voltage-dependent processes that can be determined experimentally by examining macroscopic records. We adopted the approach of Connor and Stevens (1971) and Beluzzi and Sacchi (1988), in which it is not necessary to determine separately the forward and reverse rate constants, but instead determined the time constant τ as a function of voltage. From Hodgkin and Huxley (1952) it is possible to predict time-dependent changes for each gate at a given membrane potential by knowing the voltage-dependent values of gate_∞ and τ_{gate}, in accordance with *Eq. 1*. With the given gate

$$\text{gate}_t = \text{gate}_\infty - (\text{gate}_\infty - \text{gate}_{t-1}) \exp\left(-\frac{\Delta t}{\tau_{\text{gate}}}\right) \tag{1}$$

values, normalized conductance can be calculated. We have adopted the nomenclature that Hodgkin and Huxley used for Na^+ current, and generalized it in *Eq. 2* for all inactivating conductances so that activation gate is denoted by m and the inactivation gate by h

$$\hat{g} = m^N h \tag{2}$$

The value of $\hat{g}$ is normalized to a maximum value of 1 because m and h are continuous variables between 0 and 1. Currents are obtained from Ohm's law

$$I = \hat{g} \times g_{\max} \times (E - E_{\text{Eq}}) \tag{3}$$

where $g_{\max}$ is the maximum conductance, E is the membrane potential, and E_{Eq} is the equilibrium (reversal) potential for the current. For Ca^{2+} currents, the constant-field equation was used

$$I_T = \hat{g} P z^2 \frac{EF^2}{RT} \frac{[Ca^{2+}]_i - [Ca^{2+}]_o \exp(-zFE/RT)}{1 - \exp(-zFE/RT)} \tag{4}$$

where P is the maximum permeability (in cm^3/s); z is 2 (the valence of Ca^{2+}); $[Ca^{2+}]_i$ is 10 nM; $[Ca^{2+}]_o$ is 3 mM; and E, F, R, and T have the usual meanings (Hille 1984).

To simulate voltage-dependent currents with given values of $g_{\max}$ and E_{Eq}, it is necessary to predict the value of τ_m, τ_h, h_∞, and m_∞. We have derived empirical functions that describe each of these four variables as a function of membrane potential for each of the currents studied here. Results from many experiments, which included new data as well as those from previously published studies, were collated and graphed on a common axis to demonstrate the variability in both voltage-dependent time constants and Boltzmann style "steady-state" activation and inactivation curves. Data from several cells are shown so that the range of variability can be observed. This provides a rational basis for adjusting parameters of the model within a certain range (e.g., within 1 SD of the mean). Empirical curves were fitted to the average data and then displayed on the same graphs as the raw data. The standard Boltzmann equation was used to describe both activation and inactivation

$$\frac{I}{I_{\max}} = \left\{\frac{1}{1 + \exp\left[\frac{(V - V_{1/2})}{k}\right]}\right\}^N \tag{5}$$

where $V_{1/2}$ is the membrane potential at which the channels are half (in)activated, k is the slope factor related to the valence of charge that must be displaced to switch between closed and permissive states, and N is a power factor that influences the amplitude-time course of the current (e.g., such as the "delay" of activation in voltage clamp). The power factor N may be thought of as the number of (in)activation gates, each of which must be in the permissive state for the channel to be conductive.

The rate constants for both the inactivation and activation processes were taken to be continuous functions of voltage. For the inactivation process, voltage-dependent time constants were determined either from the time constant of macroscopic current decay at suprathreshold potentials or from the time course of recovery from inactivation (deinactivation) in the subthreshold range. Activation rate was obtained from best fitted Hodgkin-Huxley curves

$$I_t = \left[1 - \exp\left(-\frac{t}{\tau_m}\right)\right]^N \exp\left(-\frac{t}{\tau_h}\right) I_\infty \tag{6}$$

where τ_m and τ_h are the activation and inactivation time constants, respectively; N is as defined above; and I_∞ is a measure of activation, i.e., the maximal current level that would be reached in the absence of inactivation (τ_h equal to infinity.). For potentials negative to activation threshold, the reverse activation process (deactivation) was determined by fitting exponential decay curves to the tail currents obtained after current activation. Because closing of each channel requires only one of the activation gates to change state, the time constant of decay of the tail current (τ_{tail}) will be $1/N$ of that for deactivation of single m gates (τ_m). For example, in the case of I_T, which is best fitted with an m^2h-type equation, the time constant of tail current decay is only half as long as the time constant of deactivation of single m gates and therefore τ_m was determined as $2 \times \tau_{\text{tail}}$ (where V_{tail} is in the membrane potential range where m_∞ approaches zero; Hagiwara and Ohmori 1982).

Data for I_T, I_A, and I_{K2} were derived from whole cell voltage-clamp studies obtained from acutely isolated ventroposterior relay neurons from young rats (7–14 days old) (Coulter et al. 1989; Huguenard et al. 1991; Huguenard and Prince 1992). With the exception of studies characterizing the temperature dependence of the ionic currents, all isolated cell experiments were performed at room temperature (23–25°C) and were compensated for capacitance and leak currents with a P/4 type subtraction protocol. Data for I_h were obtained from neurons in adult guinea pig dorsal lateral geniculate nucleus using switched-single-electrode voltage-clamp recordings with sharp electrodes in slices maintained in vitro at 35.5°C.

RESULTS

Of the multiple types of ionic current known to be present in thalamocortical relay cells, four of those that are involved in the generation of rhythmic burst discharges (I_T, I_A, I_{K2}, and I_h) have recently been characterized in detail (Coulter et al. 1989; Huguenard and Prince 1991; Huguenard et al. 1991; McCormick and Pape 1990). Here we develop mathematical descriptions of the low-threshold Ca^{2+} current I_T, the rapidly inactivating K^+ current I_A, the slowly inactivating K^+ current I_{K2}, and the hyperpolarization-activated cation current I_h for use in computational

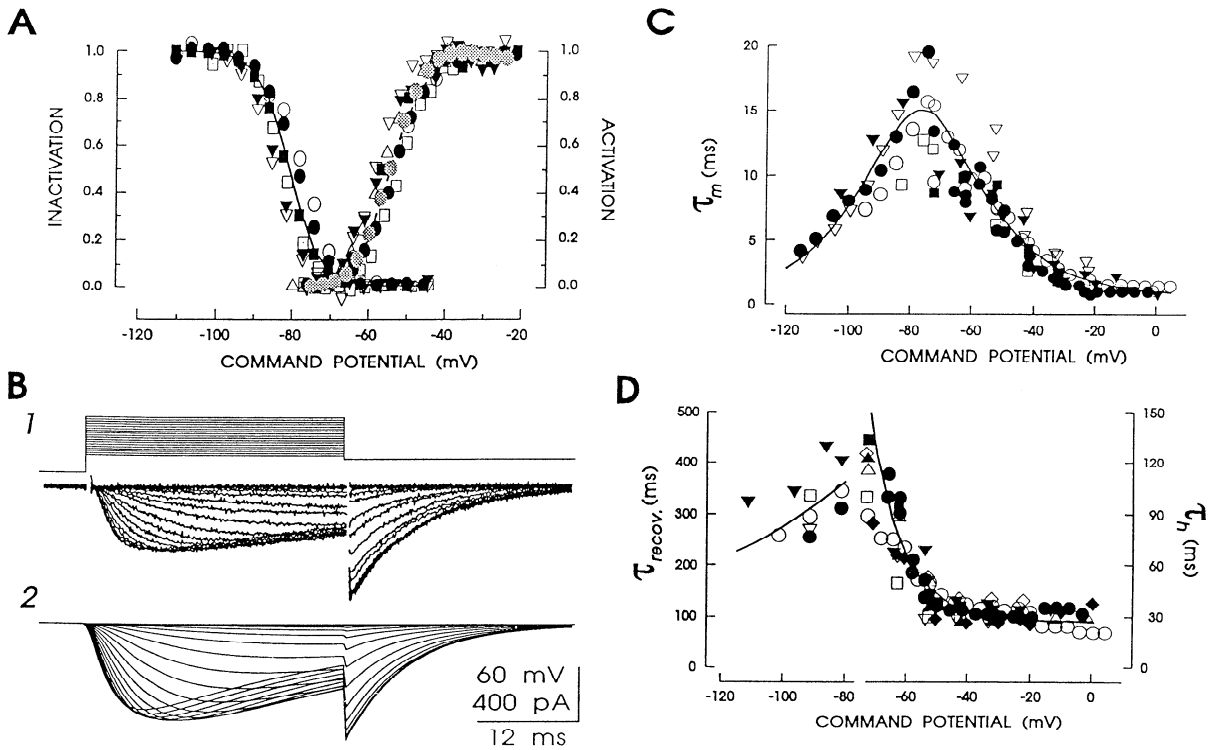

FIG. 1. Voltage-dependent activation and inactivation of I_T, as determined from voltage-clamp experiments on acutely isolated rat relay neurons. *A*: inactivation curves from 6 separate relay neurons, with average Boltzmann curve (inverse sigmoid curve, solid line). On same axes are shown the activation curve from 6 cells as determined by the tail current protocol shown in *B*. Shaded symbols are values obtained from simulation shown in *B2*, whereas the average tail current activation curve is given as dashed sigmoidal curve. *B*: activation protocol. Depolarizations of 30 ms were applied to various potentials in the activation range of I_T, followed by repolarization to −80. Tail current amplitude was then plotted as a function of depolarizing command potential in *A*. *C*: activation kinetics for I_T. Smooth bell-shaped curve is predicted by the model (*Eq. 6*). Experimental points more negative than −80 mV were obtained from tail current kinetics (see text), whereas others were determined from m^2h fits of current traces. *D*: inactivation kinetics for I_T. Points negative to −75 mV were obtained from monoexponential curves fitted to current inactivation, whereas points positive to −75 mV represent time constants of recovery from inactivation.

simulation of the electrophysiological properties of thalamocortical relay cells.

Voltage-dependent T-current models

The present mathematical description of the *T*-current was based on results obtained in parallel with a recent study that compared the properties of I_T in thalamic neurons of the reticular thalamic nucleus with those from ventroposterior relay nuclei (Huguenard and Prince 1992). In these recent studies, slightly different recording conditions were used from those of the original report on I_T in relay nuclei (Coulter et al. 1989) to improve the separation of I_T from other voltage-gated conductances. Because the results of the recent study (Huguenard and Prince 1992) provide more accurate data, these data were used in the development of the voltage-dependent model for I_T.

Normalized steady-state inactivation data from several relay cells are shown in Fig. 1*A*. We assumed that I_T was composed of a uniform population of channels whose inactivation could be completely described by the Boltzmann function (*Eq. 5*). These cells in Fig. 1 were selected from a larger population of neurons as those best fitted ($r^2 > 0.995$) to *Eq. 5* and thus deemed to be those under the most accurate voltage-clamp control. The average Boltzmann function (parameters given in Table 1) is displayed as the continuous curve. Although there was some cell-to-cell variability in the position along the voltage axis, the slope of the curve was relatively constant.

Activation functions can be obtained from fitting *Eq. 6* to the current traces obtained from depolarizations into the range of potentials where I_T is evoked (Coulter et al. 1989). However, it is necessary to know the equilibrium potential for the current to convert these curves to conductances, as is required to obtain the m_∞ curve (Hodgkin and Huxley 1952). Because obtaining the reversal potential for Ca^{2+} conductances and fitting complicated functions to experimental current traces are both somewhat unreliable proce-

TABLE 1. *Constants for Boltzmann fits of activation and inactivation*

	Inactivation		Activation		
Current	$V_{1/2}$, mV	k, mV^{-1}	$V_{1/2}$, mV	k, mV^{-1}	N
I_T	−81	4.0	−57	−6.2	2
I_{A1}	−78	6.0	−60	−8.5	4
I_{A2}	−78	6.0	−36	−20	4
I_{K2}	−58	10.6	−43	−17	1, 4
I_h			−75	5.5	1

dures, approximate activation curves were obtained with the use of tail current protocols (Fig. 1*B1*), in which the membrane potential at which activation is measured remains fixed (Hagiwara and Ohmori 1982; Regan 1991). Therefore, if we assume that the equilibrium potential is constant, then the driving force ($E - E_{Eq}$) remains fixed, and normalized tail current amplitude can be used as a measure of the *T*-channel conductance evoked by the command step.

Normalized activation curves obtained from tail current amplitudes are also shown in Fig. 1*A*. Cells were again selected on a basis of goodness of fit to *Eq. 5* with $N = 2$ and are not necessarily the same cells used for inactivation data. The dashed line is the average squared Boltzmann distribution with $V_{1/2} = -59$ mV and $k = -5.2$ mV^{-1}. The overlap of the two curves determines the membrane potential range where a window current would be persistently activated. Considering the variability in the position of the activation and inactivation curves along the voltage axis, we wanted to ensure that the degree of overlap was accurately modeled. In fact, we found that the average separation between $V_{1/2}$s for activation and inactivation curves in individual cells (22 ± 0.6 mV, $n = 17$) was identical to the separation between average $V_{1/2}$s (-81 mV to -59 mV = 22 mV).

Although tail currents amplitudes estimate activation, they do not measure the $m_\infty{}^2$ curve directly because I_T is an inactivating current. A consequence of a fixed-duration (e.g., 30 ms) depolarization is that for small depolarizations activation is not quite complete, yet for strong depolarizations significant inactivation has occurred during the step. To compensate for this inherent problem of voltage-clamp analysis of inactivating currents, we empirically chose parameters for the m_∞ curve (Table 1) in the model that resulted in a simulated tail current activation curve (Fig. 1*B2*, and gray shaded symbols in Fig. 1*A*) equivalent to that obtained with neurons. This method presumably results in a more accurate description of the Boltzmann activation function that describes I_T.

Activation kinetics for I_T displayed a bell-shaped voltage dependency (Fig. 1*C*) similar to that seen for Na^+ and K^+ currents (Hodgkin and Huxley 1952). The smooth curve is drawn according to

$$\tau_m = \frac{1}{\exp\left(\frac{V_m + 132}{-16.7}\right) + \exp\left(\frac{V_m + 16.8}{18.2}\right)} + 0.612 \qquad (7)$$

Inactivation kinetics for I_T were biphasic. Recovery from inactivation occurred at much slower rates (250–400 ms at potentials between -100 and -80 mV, Fig. 1*D*) than current inactivation (25–130 ms in the range of -75–0 mV, Fig. 1*D*). It was thus difficult to obtain a simple continuous function that described the voltage dependence of the inactivation time constant (τ_h), and two separate functions were derived and are presented in *Eq. 8*.

$$V_m < -80 \text{ mV} \quad \tau_h = \exp\left(\frac{V_m + 467}{66.6}\right)$$

$$V_m \geq -80 \text{ mV} \quad \tau_h = \exp\left(\frac{V_m + 22}{-10.5}\right) + 28 \qquad (8)$$

The fitted curve at hyperpolarized potentials was chosen to reflect the slope of the voltage-dependent recovery process within cells, rather than to attempt to obtain a curve fitted to all data points in which case the slope describing recovery would be too shallow at hyperpolarized membrane potentials.

Simulations of T-current

Simulations were performed to test whether the voltage-dependent models for I_T could reproduce voltage-clamp results obtained from relay neurons. Time- and voltage-dependent values of m and h were calculated based on *Eq. 1*, and currents were then obtained from the constant-field equation (*Eq. 4*). Families of currents generated by this means reproduced both the time course and amplitude of actual current traces (Fig. 2*A*). Peak current amplitude was negligible below -70 mV and gradually increased as the command step was made more positive. Maximum peak current occurred near -38 mV in both the example relay neuron and the simulation (Fig. 2*B1*). On the other hand, the peak current-voltage (*I-V*) relationship could not be accurately reproduced when an ohmic relation between voltage, current, and *T*-conductance (*Eq. 3*) was used rather than the constant-field equation (*Eq. 4*). For example, with the ohmic equation, the maximal amplitude occurred at more depolarized potentials and exhibited very gradual reductions with further depolarizations in comparison with the constant-field relation and the actual data. Notably, the model was able to accurately reproduce peak current amplitudes (Fig. 2*B2*).

Initial reports indicated that recovery from inactivation of I_T was biexponential in relay neurons (Coulter et al. 1989). However, using the voltage protocol shown in Fig. 2*C*, we have found that recovery could be described by a monoexponential process. Here the holding membrane potential is set to -40 mV to completely inactivate I_T (see Fig. 1*A*). After brief hyperpolarization to -90 mV, a small I_T was activated on return to -40 mV and current amplitude increased as the hyperpolarization was lengthened. The time course of recovery from inactivation was well described as an exponential process with τ_{recov} equal to 300 ms at this membrane potential (dashed line). The simulation model reproduced this result (Fig. 2*C3*). In other experiments, varying the step potential from -110 to -80 mV revealed τ_{recov} to vary in a voltage-dependent manner, as modeled by *Eq. 8* above (not shown).

Voltage-dependent A-current models

A prominent current in isolated thalamocortical relay neurons is the rapidly inactivating K^+ current known as I_A (Huguenard et al. 1991). Steady-state inactivation data for I_A from several cells (Fig. 3*A*) show that there was clustering of many values near the mean. However, occasionally there were variants (e.g., ○ in Fig. 3*A*). This may reflect the fact that ventroposterior relay neurons are not a uniform population of cells, as far as transient K^+ currents are concerned. Nevertheless, we have developed a model of I_A in the "average" relay neuron. The smooth curve is the aver-

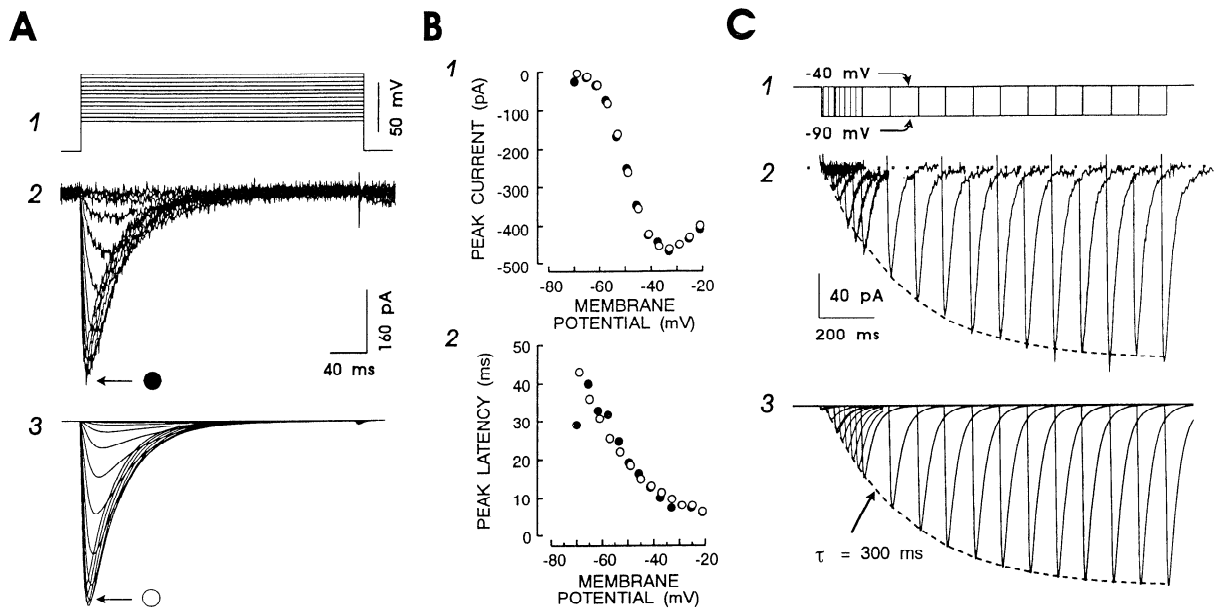

FIG. 2. Simulation of voltage-dependent I_T activation and recovery from inactivation. *A*: current traces in a typical relay neuron compared with simulated currents. *1*: voltage protocol. Holding membrane potential was −100 mV, and 300-ms step depolarizations to potentials in the range of −74 to −26 mV were applied. *2*: resultant currents obtained from voltage-clamp recordings in a relay neuron. *3*: simulation results. *B*: comparison between cell and model. *1*: current-voltage (*I-V*) relationship for peak I_T in the real neuron (●) and the simulation results (○). *2*: peak latency as a function of membrane potential for I_T in real neuron (●) and the simulation (○). *C*: simulation of recovery from inactivation for I_T. *1*: voltage protocol in which holding membrane potential was set at −40 mV to inactivate I_T and hyperpolarizations to −90 mV of increasing durations (5–1,600 ms) were applied. *2*: current traces obtained from a representative relay neuron. *T*-current was virtually nonexistent with very short conditioning pulses and then asymptotically approached a plateau level as the conditioning step was lengthened. Dotted line indicates holding current at −40 mV, and the dashed line is an exponential decay curve with a time constant (τ) of 300 ms. *3*: results of voltage-clamp simulation with same voltage protocol as in *B*.

age Boltzmann curve for steady-state inactivation in four cells with similar properties (Fig. 3*A*; parameters given in Table 1).

Activation of I_A was more difficult to describe than inactivation, in that a simple Boltzmann curve could not be well fitted to the data. One explanation consistent with these results is that "I_A" is actually composed of two different populations of voltage-gated channels. We empirically modeled I_A as the sum of two independent currents with comparable activation kinetics and steady-state inactivation. In support of the hypothesis of two populations of channels was the finding that the time course of I_A inactivation was biexponential, and the proportion of the slow and fast decaying components changes as a function of voltage (Huguenard et al. 1991). The gray circles in Fig. 3*A* are the results of simulation in which the tail current activation curve was obtained. The simulated current was modeled as the sum of two currents (I_{A1} and I_{A2}) with parameters given in Table 1 and with the more rapidly decaying component, I_{A1}, accounting for 60% of the total I_A conductance. With the two activation curves (Table 1) having different voltage dependencies, small depolarizations favor activation of I_{A1}, whereas stronger depolarizations activate increasing proportions of I_{A2}, as was reported for whole cell I_A (Huguenard et al. 1991).

Activation kinetics for I_A (Fig. 3*C*) were obtained by fitting current traces to *Eq. 6* with $N = 4$ (Huguenard et al. 1991), and deactivation rates at potentials less than −60 mV were estimated by dividing tail current time constant by 4. Activation time constant displayed a bell-shaped dependence on voltage that was described by

$$\tau_m = \frac{1}{\exp\left(\frac{V_m + 35.8}{19.7}\right) + \exp\left(\frac{V_m + 79.7}{-12.7}\right)} + 0.37 \qquad (9)$$

and plotted as the continuous curve in Fig. 3*C*. As indicated previously, inactivation of I_A proceeded with two decay time constants, and the slower component became more prominent with stronger depolarizations. However, both time constants were independent of membrane potential (Fig. 3*D*). In contrast, the rate of recovery from inactivation was highly voltage sensitive (Fig. 3*D*), with time constant values varying between 12 and 65 ms in the range of −140 to −80 mV. The smooth curve in Fig. 3*D* is drawn according to

$$V_m < -63 \text{ mV} \quad \tau_{h1} = \frac{1}{\exp\left(\frac{V_m + 46}{5.0}\right) + \exp\left(\frac{V_m + 238}{-37.5}\right)}$$

$$V_m \geq -63 \text{ mV} \quad \tau_{h1} = 19 \qquad (10)$$

The kinetics of removal of inactivation for the slower component (τ_{h2}) were similar to those for τ_{h1}, but inactivation occurred with a slower, but constant rate. Therefore, for membrane potentials less than −73 mV, τ_{h2} was modeled as being equal to τ_{h1} and at other potentials was 60 ms.

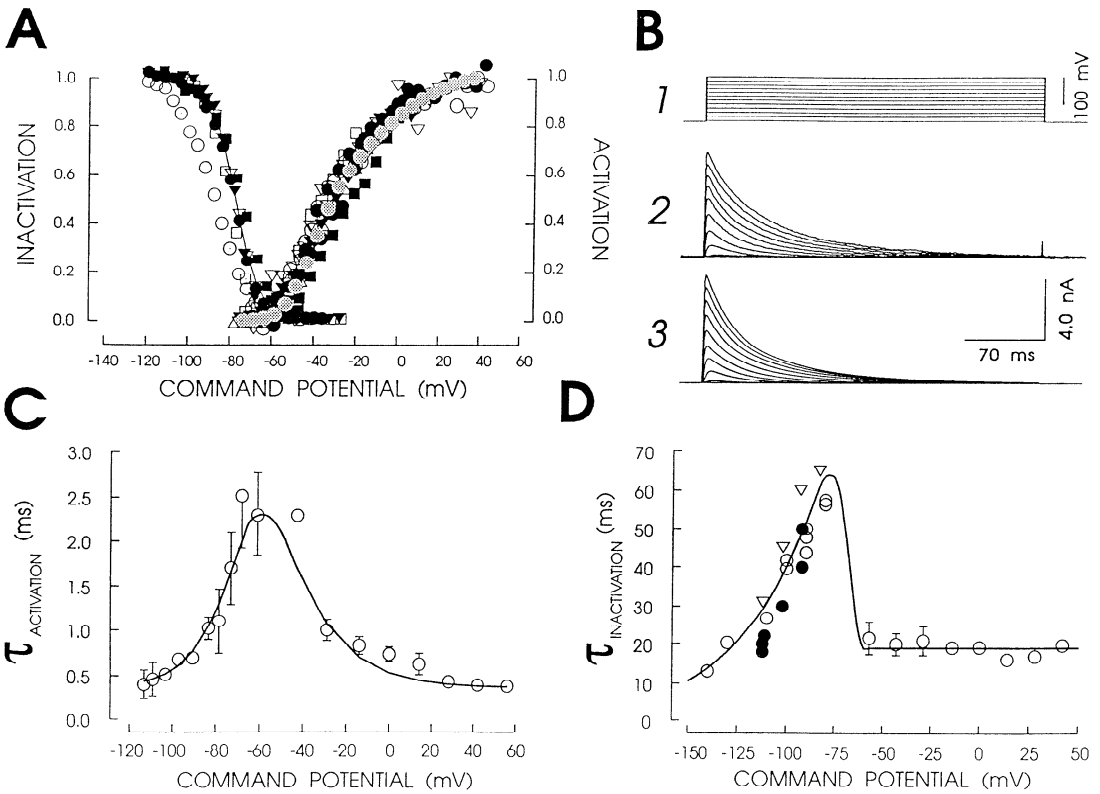

FIG. 3. Voltage-dependent gating of I_A. *A*: steady-state activation and inactivation curves. Inactivation data are from standard steady-state inactivation protocols in which depolarizations to 0 mV were preceded by 1-s conditioning pulses in the range of −120 to −25 mV. Continuous curve is the average fitted Boltzmann curve that was used in the model. Activation data are from tail current protocols in which 4-AP–sensitive current activated by 4-ms depolarization in the range of −74 to +36 mV, followed by returning the potential to −70 mV, at which point tail current amplitude was measured at a latency of 0.2 ms. Gray shaded circles are those obtained by simulation. *B*: normal vs. simulated I_A. *1*: voltage protocol, in which 300-ms depolarizations to membrane potentials between −96 and +58 mV from a holding potential of −100 mV. *2*: example I_A activation in a relay neuron. *3*: simulation results. *C*: activation kinetics and model fit for I_A. Data points for values negative to −60 mV were obtained from deactivation (tail current) kinetics, whereas points positive to −60 mV are the results of currents fitted by the m^4h-protocol (see RESULTS). *D*: inactivation kinetics and model fit for I_A. Inactivation measured as whole cell current decay was voltage independent in the range of −60 to +40 mV. On the other hand, deinactivation as measured by the time course of recovery from inactivation at potentials between −80 and −140 mV was highly voltage dependent. Relay neuron data in all panels from results of Huguenard et al. (1991).

Simulations of A-current

The A-current was described as the sum of a rapidly (I_{A1}) and more slowly (I_{A2}) inactivating components. Each subcomponent (I_{A1} and I_{A2}) was described by *Eqs. 2* and *3* with $N = 4$ and g_{maxA1} varying between 11.2 and 50 nS while g_{maxA2} varied from 7.5 to 33 nS. Voltage-clamp simulations (Fig. 3*B*) reproduced the essential features of I_A. Currents activated rapidly on depolarization, and then inactivated; as the command potential was increased, peak current occurred earlier and the slower decay component became more prominent.

Voltage-dependent models for I_{K2}

Application of depolarizing voltage steps to isolated thalamocortical relay neurons reveals a second inactivating K^+ current that is sensitive to block by tetraethylammonium (TEA) and that has been termed I_{K2} (Huguenard and Prince 1991). The steady-state activation curve for I_{K2} displays a threshold of approximately −60 mV and extends across a broad voltage range up to +30 mV (Fig. 4*A*). The slowly increasing slope of the activation curve at membrane potentials between −60 and −30 mV made this curve difficult to fit with a simple Boltzmann equation with N equal to 1. Increasing N to 4 greatly increased the accuracy of the fit, particularly at these membrane potentials. However, examination of the time course of activation of I_{K2} does not reveal any substantial delay or "S" shape during activation (Fig. 4*D2*), as would be expected for m^4h-type kinetics. We therefore chose different values of N to accurately model both activation rate (*Eq. 6* with $N = 1$) and steady-state activation (*Eq. 5* with $N = 4$). This compromise yielded reasonable simulations for both amplitude and time course of I_{K2} (Fig. 4*C*).

A recent investigation of I_{K2} suggested that this current may display incomplete steady-state inactivation (Fig. 4*A*; Huguenard and Prince 1991). However, this incomplete inactivation may have resulted from the duration of the inactivating voltage steps used in this experiment (2 s) being of insufficient duration to allow complete inactivation of this slowly inactivating current (see below). Here we have modeled I_{K2} as a completely inactivating current with

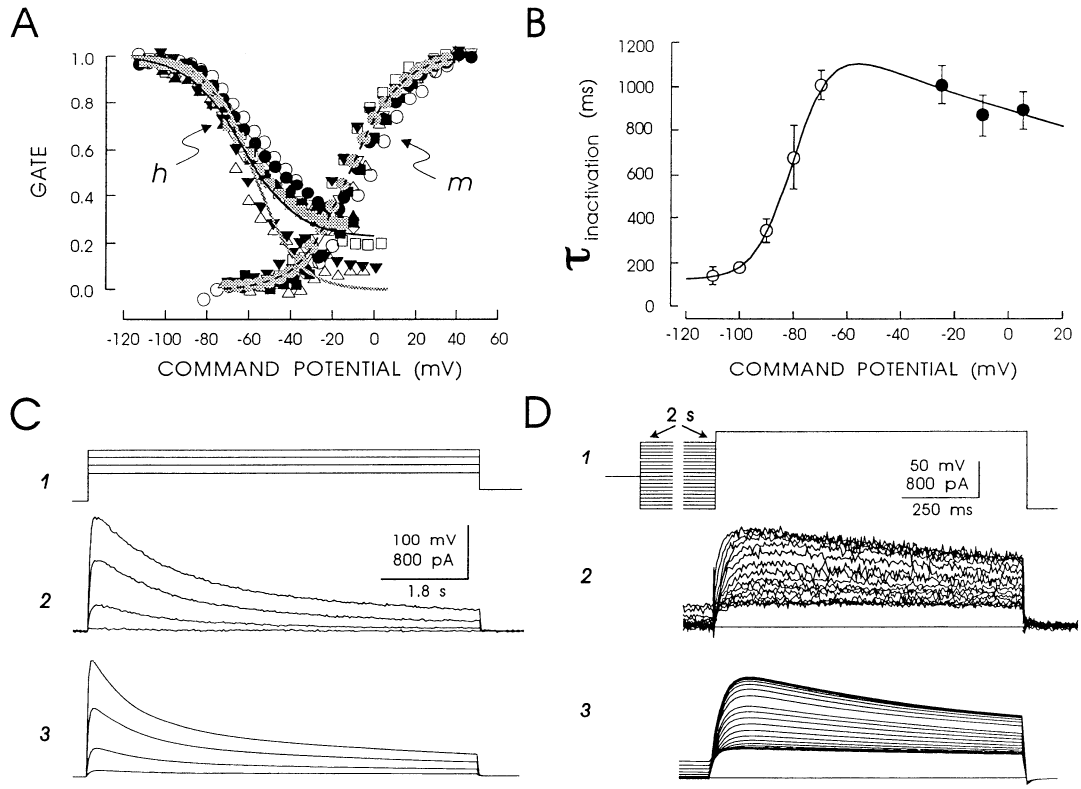

FIG. 4. Voltage-dependent gating of the slowly inactivating K^+ current (I_{K2}) in relay neurons. Based on voltage-clamp data obtained in a previous study (Huguenard and Prince 1991). *A*: steady-state inactivation (h) and tail current activation (m) obtained in several cells. Notice variable and incomplete inactivation. Gray symbols are results of the simulation in both activation and inactivation curves. Solid black curve is the average fitted Boltzmann curve for "steady-state inactivation" with the given protocol, whereas true steady-state inactivation is shown as the gray continuous line. Discontinuous line is the average activation curve. *B*: voltage-dependent kinetics of inactivation of I_{K2} with modeled curve. Open symbols are from the time constant of recovery from inactivation, whereas closed symbols are the faster of 2 components of decay seen with I_{K2}. *C*: simulation of I_{K2} time course. *1*: voltage protocol in which 5-s depolarizations are applied to −40, −25, −10, and +5 mV from and holding potential of −90 mV. *2*: voltage-clamp current (TEA-sensitive) from a typical relay neuron. *3*: simulation currents from the model. *D*: "steady-state" inactivation. *1*: voltage-clamp protocol in which 1-s depolarizations to 0 mV were preceded by 2-s conditioning pulses in the range of −110 to −15 mV. *2*: typical results obtained from a relay neuron for TEA-sensitive current. Note that current during the conditioning pulse is nonzero during the most depolarized conditioning potentials and also that the test current is not fully inactivated even at the most depolarized conditioning potentials. See text for further discussion. *3*: simulation obtained with the same voltage protocol.

two time constants of inactivation, as for I_A. However, for I_{K2} the proportion of the two decay components was not dependent on voltage. Therefore the parameters for steady-state activation and inactivation curves (Table 1) were taken to be the same for both components, I_{K2a} and I_{K2b}, and the faster decay component was modeled as accounting for 60% of the total. Activation time constants for both I_{K2a} and I_{K2b} (see Fig. 4*D* in Huguenard and Prince 1991) were fitted to

$$\tau_m = \frac{1}{\exp\left(\frac{V_m - 81}{25.6}\right) + \exp\left(\frac{V_m + 132}{-18.0}\right)} + 9.9 \qquad (11)$$

and inactivation kinetics of the fast component, I_{K2a}, were modeled by

$$\tau_h = \frac{1}{\exp\left(\frac{V_m - 1{,}329}{200}\right) + \exp\left(\frac{V_m + 130}{-7.1}\right)} + 120 \qquad (12)$$

which is shown as the smooth curve in Fig. 4*B*. The inactivation kinetics for the slower component, I_{K2b}, were taken to be the same as for I_{K2a} at potentials negative to −70 mV (i.e., for recovery from inactivation) and 8.9 s at more depolarized levels (Huguenard and Prince 1991).

Simulations of I_{K2}

As for the rapidly inactivating K^+ current I_A, the slowly inactivating K^+ current I_{K2} was modeled as the sum of two components (I_{K2a} and I_{K2b}) that inactivate at different rates. Each component was modeled according to *Eqs. 2* and *3* with $N = 1$ and maximal conductances ranging between 6.4 and 39 nS for g_{maxK2a} and 4.3 and 26 nS for g_{maxK2b}. Simulated currents reproduced the important features of the experimental data. Tail current activation protocols accurately simulated (gray circles in Fig. 4*A*) the results from relay neurons. In addition, simulated I_{K2} had a relatively long latency to peak that was best fitted with a m^1h relation as in the original report (Huguenard and Prince 1991), and the current decayed with two time con-

stants near 1 and 10 s at room temperature (Fig. 4*C*). During simulations of the voltage-clamp behavior of I_{K2}, we found that the apparent incomplete inactivation obtained with the original steady-state protocols (Huguenard and Prince 1991) was probably a consequence of using an insufficiently long conditioning pulse (2 s was typically used), so that the I_{K2} channels were not at true steady state. Simulations obtained with the same protocol reproduced the apparent incomplete inactivation (Fig. 4*D* and gray squares in Fig. 4*A*), whereas true steady-state inactivation protocols produced complete inactivation (shaded inactivation line in Fig. 4*A*).

Voltage-dependent h-current model

Mathematical description of the *h*-current was derived from data obtained with voltage-clamp recordings of guinea pig dorsal lateral geniculate relay neurons maintained in vitro as a thalamocortical slice (McCormick and Pape 1990). Analysis of tail currents during activation of I_h (Fig. 5*C*) revealed an activation curve that was well fitted by *Eq. 5* with a $V_{1/2}$ of −75 mV and a slope factor k of 5.5 mV^{-1} (Table I). The *h*-current does not inactivate, even with prolonged (minutes) hyperpolarization (McCormick and Pape 1990). The time constants of activation and deactivation of I_h were well fitted ($r > 0.95$) by single exponential functions. The rate of activation and deactivation of I_h was modeled as a bell-shaped function (Fig. 5*B*) according to

$$\tau_m = \frac{1}{[\exp(-14.59 - 0.086\ V_m) + \exp(-1.87 + 0.0701\ V_m)]} \quad (13)$$

Simulations of h-current

Simulations of the response of thalamocortical relay cells to hyperpolarizing current pulses at a temperature of 35.5°C were performed to examine the accuracy of the mathematical model of I_h. Because the model is based on non–leak-subtracted data (e.g., Fig. 5*C*), a leak conductance (see McCormick and Huguenard 1992) was also included in the simulation. The *h*-current was described by *Eqs. 2* and *3* where $N = 1$, $h = 1$ (no inactivation), E_{Eq} was −43 mV, and g_{max} was between 15 and 30 nS (McCormick and Pape 1990). The single power factor ($N = 1$) for activa-

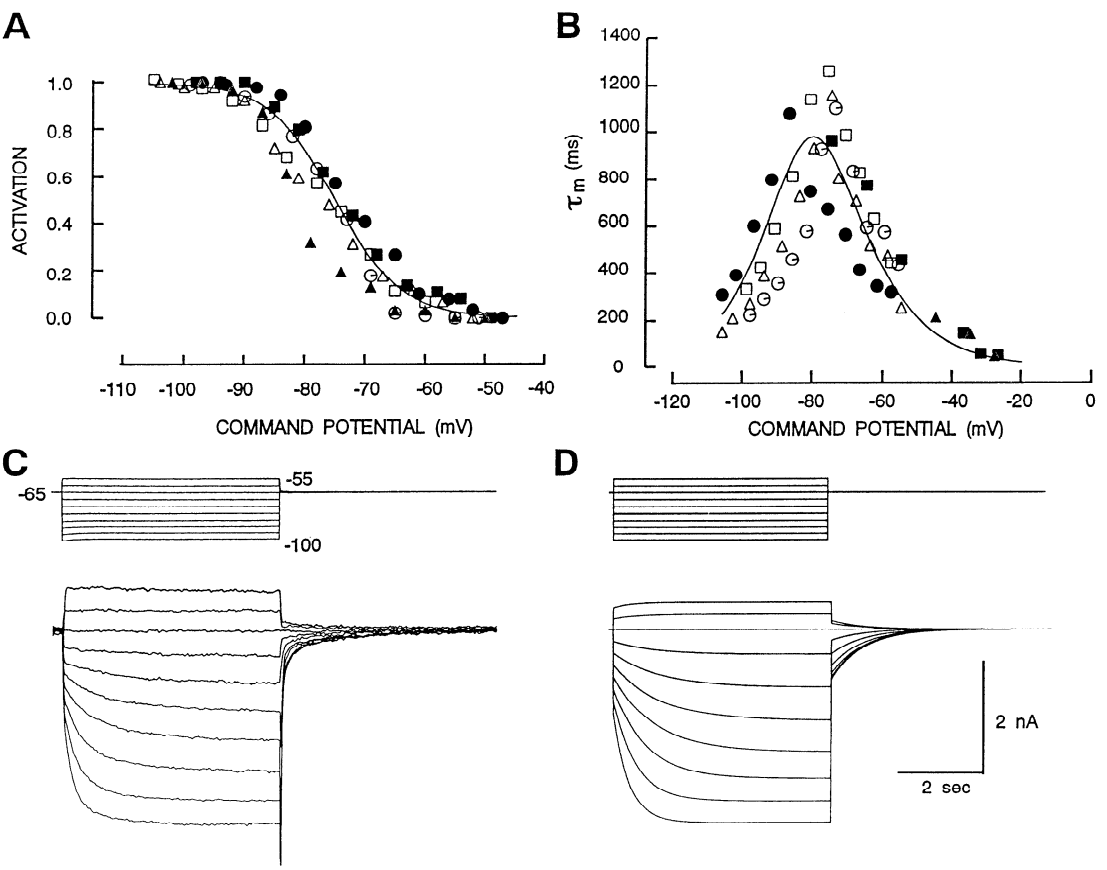

FIG. 5. Voltage-dependent properties and simulation of the hyperpolarization-activated cation current I_h. *A*: activation curve for I_h as determined from 6 different guinea pig lateral geniculate relay neurons. Activation data points were obtained from measurement of the slowly decaying components of tail currents, which appear after stepping to various hyperpolarized membrane potentials (e.g., *C*). Solid line is the Boltzmann fit of these data. *B*: kinetics of activation and deactivation of I_h determined in 6 different guinea pig relay neurons. Solid line is the mathematical description of these data. *C*: stepping for 5 s to membrane potentials from −55 to −100 mV illustrates the activation of I_h. *D*: simulation of I_h. At the holding potential of −65 mV, a small amount of I_h is active, which deactivates on stepping to −55 mV. Hyperpolarization to more negative membrane potentials progressively activates I_h and changes the time constant of activation. Stepping back to −65 mV illustrates the tail currents generated by I_h deactivation.

tion appears to be justified, given the lack of an apparent delay in the activation of I_h (Fig. 5*A*). Comparison of voltage-clamp recordings from guinea pig thalamocortical relay cells (Fig. 5*C*) with the results of the simulation (Fig. 5*D*) reveal several similarities including the voltage dependence and kinetics of activation and deactivation. The presence of an additional, faster component to the tail currents during deactivation of I_h in guinea pig dorsal lateral geniculate nucleus cells (Fig. 5*C*) is due to the presence of I_T, which was not blocked in these biological experiments (McCormick and Pape 1990).

DISCUSSION

Detailed descriptions of the electrophysiological properties of neurons require a thorough investigation of the properties of the underlying currents, their spatial localization, and their sensitivity to alteration from intracellular and extracellular signals. Here we have formulated mathematical descriptions of four ionic currents present in thalamocortical relay cells, using the methods pioneered by Hodgkin and Huxley (1952). These four ionic currents, I_T, I_A, I_{K2}, and I_h, were chosen on the basis of their robust presence in thalamocortical relay neurons, their probable contribution to the ability of thalamic relay neurons to generate rhythmic burst discharges, and their presence at membrane potentials at or near rest and action potential threshold.

T-current

The low-threshold Ca^{2+} current, or *T*-current, is likely to be the main inward current in the production of low-threshold Ca^{2+} spikes (LTS; Llinás and Jahnsen 1982). A number of notable features of I_T are replicated in the present mathematical model, which predicts a dominant contribution of this current to the generation of low-threshold Ca^{2+} spikes. First, the voltage dependence of I_T activation is in the membrane potential range of −70 to −40 mV, and inactivation occurs at membrane potentials between −90 and −60 mV in similarity with the activation and inactivation range of the low-threshold Ca^{2+} spike (see Jahnsen and Llinás 1984a,b). Second, the rate of activation of I_T is considerably more rapid than its rate of inactivation (e.g., Fig. 1, *C* and *D*), a property that should facilitate the generation of prolonged (10s of ms) low-threshold Ca^{2+} spikes. The near completeness of steady-state inactivation at normal resting membrane potentials (−63 mV) for rodent thalamocortical relay neurons and the position of the inactivation and activation curves on the voltage axis for I_T (see Fig. 1*A*) further predict that thalamocortical relay neurons at this membrane potential are ideally situated to respond to hyperpolarizing inputs, whether induced by current injection or by inhibitory postsynaptic potentials, with a rebound Ca^{2+} spike-mediated burst of action potentials, as found in vitro and in vivo (Deschênes et al. 1982; Jahnsen and Llinás 1984a,b). The rate of removal of inactivation found here was well described by a single exponential function, in contrast to previous voltage-clamp data (Coulter et al. 1989) and a computational model based on this data (Wang et al. 1991). Furthermore, the model presented here predicts a time constant for removal of inactivation of near 70 ms at −90 mV and at physiological temperatures (e.g., 37°C). This slow time course suggests that decreasing the interval between low-threshold Ca^{2+} spikes to less than ~500 ms will result in significant decreases in the amplitude of each Ca^{2+} spike (other than the first), as is found in rodent thalamocortical relay neurons in vitro (McCormick and Feeser 1990). In addition, although it will depend critically on the amplitude and distribution of I_T and other biophysical features of thalamocortical relay cells, this rate of removal of inactivation suggests that thalamocortical relay cells may not be capable of generating rhythmic low-threshold Ca^{2+} spikes at frequencies in excess of ~12–14 Hz, a prediction that is in good agreement with the highest frequency of rhythmic low-threshold Ca^{2+} spike generation in vivo (Shosaku et al. 1989; Steriade and Deschênes 1984).

Although the contribution of I_T to the generation of low-threshold Ca^{2+} spikes is now well established, the voltage dependency and kinetics of this current suggest that it may also contribute to other electrophysiological properties of thalamic relay cells. For example, the presence of a small degree of overlap in the activation and inactivation curves for I_T suggests that this current may exhibit a steady, but small, activation at certain membrane potentials (e.g., around −70 mV), which may facilitate a tonic depolarization of these neurons at or near resting membrane potentials. In addition, the presence of large (10–20 mV) and prolonged (up to 60 ms) hyperpolarizations after the generation of single action potentials suggests that these hyperpolarizations may be of sufficient amplitude to partially remove inactivation of I_T, thereby allowing this current to contribute to the generation of single spike activity, a hypothesis that remains to be tested in thalamocortical relay neurons. The predicted slow time course of I_T-mediated Ca^{2+} spikes and the extension of activation up to −40 mV suggests that these events may activate not only the Na^+ and K^+ currents involved in the generation of action potentials, but also the rapidly and slowly inactivating K^+ currents I_A and I_{K2}. The actions of these currents, in turn, may modulate the amplitude-time course of low-threshold Ca^{2+} spikes.

A-current

The voltage-dependent and kinetic properties of I_A suggest that this current may contribute to both low-threshold Ca^{2+} spikes and fast Na^+ spikes. In particular, the slower rate of activation of I_T in comparison with I_A and the activation threshold of I_A of around −60 mV (cf. Figs. 1*C* and 4*C*) suggests that I_A may have considerable effects on the rising phase of low-threshold Ca^{2+} spikes. In addition, the activation kinetics of I_A are probably sufficiently fast to allow contribution to the repolarization of Na^+-dependent action potentials, as has been hypothesized in other neuronal cell types (see Storm 1990). Although the kinetics of inactivation are complex, they could be accurately reproduced by assuming the whole cell I_A to be composed of two separate conductance mechanisms (Table I). Because I_A inactivates rapidly (with τ values near 4 and 15 ms at −40 mV and 37°C) it probably does not contribute to regulating

rhythmic LTS activity, but on the other hand it can contribute to shaping the amplitude-time course of LTSs. In addition, the movement of the membrane potential between −50 and −70 mV during the generation of Na^+-dependent action potentials also suggests that activation of I_A may contribute to the control of repetitive firing (e.g., Connor and Stevens 1971). The lack of substantial overlap of the steady-state activation and inactivation curves for I_A suggests that this current is not likely to contribute strongly to "tonic" properties of thalamocortical relay cells, such as resting membrane potential and input resistance.

Slowly inactivating K-current, I_{K2}

The slowly inactivating K^+-current, I_{K2}, displays a number of interesting features. Both the membrane potential range of activation and inactivation extend through large parts of the voltage axis. The membrane potential range of activation extends from below Na^+ spike firing threshold (approximately −55 mV) to membrane potentials positive to 0 mV (Fig. 5*A*), whereas inactivation extends from −100 mV up to membrane potentials substantially positive to firing threshold (e.g., up to −20 mV). The kinetics of inactivation of this current are quite slow, with time constants near 300 and 2,500 ms at physiological temperature, whereas the kinetics of activation are substantially faster. These properties predict that I_{K2} will contribute substantially to the amplitude-time course of low-threshold Ca^{2+} spikes and may contribute to their repolarization, a prediction confirmed in the accompanying paper (McCormick and Huguenard 1992). In addition, the activation threshold of I_{K2} at membrane potentials negative to firing threshold suggests that this current may retard the approach of the membrane potential toward the activation of action potentials on depolarization. Although the above hypotheses remain to be tested in thalamocortical relay neurons, recent intracellular recordings in vitro from guinea pig dorsal lateral geniculate nucleus cells have revealed the presence of a current, called I_{As}, which also activates in the same voltage range and inactivates with a time course similar to I_{K2} (100s ms to s; McCormick 1991). Pharmacological examination of the functional contribution of I_{As} to the firing properties of thalamic relay cells suggests that this current generates a substantial delay on depolarization to the onset of action potential discharge and also contributes to the repolarization of the low-threshold Ca^{2+} spike (McCormick 1991). Therefore, functionally, I_{K2} and I_{As} appear to have a number of similarities. However, a substantial difference between these currents is that I_{K2} is sensitive to block by TEA and not 4-aminopyridine (4-AP), whereas I_{As} is highly sensitive to 4-AP but not TEA (Huguenard and Prince 1991; McCormick 1991). The possible presence of two slowly inactivating K^+ currents in thalamocortical relay neurons with very similar voltage-dependent characteristics remains to be examined in more detail.

In addition to modulating the response of thalamocortical relay neurons to tonic depolarization, the kinetics and voltage-dependent properties of I_{K2} also suggest that this current may be involved in the control of repetitive single spike activity, particularly in between sequential Na^+ spikes, in a manner similar to I_A. However, the slow kinetics of I_{K2} suggest that this current may exhibit only small changes in activation and inactivation during the generation of action potentials, even though it may strongly affect the pattern of action potentials generated (see McCormick and Huguenard 1992).

H-current

The voltage dependence of activation of the hyperpolarization-activated cation current I_h was well fitted by a Boltzmann equation, whereas the kinetics of activation and deactivation appeared as a bell-shaped curve centered around half activation. These properties of I_h are remarkably similar to those of the hyperpolarization-activated cation current I_f present in single sinoatrial cells (e.g., Nobel et al. 1989). In these cells, I_f is believed to contribute to the generation of the "pacemaker" potential, i.e., the flow of ions that drives the membrane toward the threshold for generation of each action potential (see DiFrancesco 1985). Similarly, the properties of I_h modeled here predict that hyperpolarization of thalamic relay neurons will result in a repolarization of the membrane to more depolarized levels, thereby resulting in a depolarizing "sag." The amplitude-time course of this depolarization will depend on the degree of hyperpolarization, because increasing the hyperpolarization will result in a stronger and more rapid activation of I_h (e.g., Fig. 7, *A* and *B*). Recent intracellular recordings in cat lateral geniculate relay neurons reveal the presence of a Cs^+-sensitive "pacemaker" potential in between the generation of low-threshold Ca^{2+} spikes, suggesting that I_h may contribute to the generation of slow, rhythmic burst firing (McCormick and Pape 1990; Soltesz et al. 1991). This hypothesis is confirmed and extended in the accompanying paper on the basis of the mathematical description of I_h developed here (McCormick and Huguenard 1992).

Limitations of the models of ionic currents

We have attempted to develop mathematical descriptions of four different currents that exist in thalamocortical relay neurons. These descriptions are useful in predicting the amplitude-time course of each of these currents given a complicated voltage trajectory, such as that which occurs in neurons during the generation of action potentials. However, the models also have limitations. First, the spatial distribution of the different ionic currents in thalamocortical relay cells is for the most part unknown and may have important consequences on the activity of these cells and their response to synaptic inputs. Second, we have considered thalamocortical relay neurons of different sensory and motor nuclei to be composed of a relatively homogenous population. Heterogeneity among different relay cells in different nuclei (e.g., McCormick and Prince 1988) or within the same nucleus (Bloomfield et al. 1987; Mastronarde 1987) may have important functional consequences (e.g., the presence or absence or rhythmic burst discharges or "lagged" visual responses). Third, the dynamics of Ca^{2+} buffering in thalamic relay neurons have not yet been investigated. Finally, the present model of ionic currents is of only limited

value in describing the properties of the single ionic channels that underlie these currents, which, at least in the case of I_A and I_{K2}, may themselves be composed of a wide variety of subtypes of channels. However, despite these and other potential problems, the present simulations of whole cell currents in thalamocortical relay cells are capable of reconstructing many of the basic electrophysiological features of these neurons (McCormick and Huguenard 1992) and therefore are of value in understanding the physiological properties of thalamic function.

This work was supported by National Institute of Neurological Disorders and Stroke Grants NS-06477 and NS-12151 to D. A. Prince and NS-26143 to D. A. McCormick. D. A. McCormick was also supported by the Klingenstein Fund and the Sloan Foundation.

Address for reprint requests: J. R. Huguenard, Dept. of Neurology and Neurological Sciences, Room M016, Stanford University Medical Center, Stanford, CA 94305-5300.

Received 24 March 1992; accepted in final form 8 June 1992.

REFERENCES

BELLUZZI, O. AND SACCHI, O. The interactions between potassium and sodium currents in generating action potentials in the rat sympathetic neuron. *J. Physiol. Lond.* 397: 127–147, 1988.

BLOOMFIELD, S. A., HAMOS, J. E., AND SHERMAN, S. M. Passive cable properties and morphological correlates of neurons in the lateral geniculate nucleus of the cat. *J. Physiol. Lond.* 383: 653–692, 1987.

CONNOR, J. A. AND STEVENS, C. F. Prediction of repetitive firing behaviour from voltage clamp data on an isolated neuron soma. *J. Physiol. Lond.* 213: 31–53, 1971.

COULTER, D. A., HUGUENARD, J. R., AND PRINCE, D. A. Calcium currents in rat thalamocortical relay neurons: kinetic properties of the transient, low-threshold current. *J. Physiol. Lond.* 414: 587–604, 1989.

CRUNELLI, V., LIGHTOWLER, S., AND POLLARD, C. A T type calcium current underlies the low threshold calcium potential in cells of the cat and rat lateral geniculate nucleus. *J. Physiol. Lond.* 413: 543–561, 1989.

DESCHÊNES, M., ROY, J. P., AND STERIADE, M. Thalamic bursting mechanism: an inward slow current revealed by membrane hyperpolarization. *Brain Res.* 239: 289–293, 1982.

DIFRANCESCO, D. The cardiac hyperpolarizing-activated current I_f: origin and developments. *Prog. Biophys. Mol. Biol.* 46: 163–183, 1985.

DIFRANCESCO, D. AND NOBLE, D. A model of cardiac electrical activity incorporating ionic pumps and concentration changes. *Philos. Trans. R. Soc. Lond. B Biol. Sci.* 307: 353–398, 1985.

DIFRANCESCO, D. AND NOBLE, D. Current I_f and its contribution to cardiac pacemaking. In: *Neuronal and Cellular Oscillators,* edited by J. W. Jacklet. New York: Dekker, 1989, p. 31–57.

HAGIWARA, S. AND OHMORI, H. Studies of calcium channels in rat clonal pituitary cells with patch electrode voltage clamp. *J. Physiol. Lond.* 331: 231–252, 1982.

HERNÁNDEZ-CRUZ, A. AND PAPE, H.-C. Identification of two calcium currents in acutely dissociated neurons from the rat lateral geniculate nucleus. *J. Neurophysiol.* 61: 1270–1283, 1989.

HILLE, B. *Ionic Channels of Excitable Membranes.* Sunderland, MA: Sinauer, 1984.

HODGKIN, A. L. AND HUXLEY, A. F. A quantitative description of membrane current and its application to conduction and excitation in nerve. *J. Physiol. Lond.* 117: 500–544, 1952.

HUGUENARD, J. R., COULTER, D. A., AND PRINCE, D. A. A fast transient potassium current in thalamic relay neurons: kinetics of activation and inactivation. *J. Neurophysiol.* 66: 1304–1315, 1991.

HUGUENARD, J. R., HAMILL, O. P., AND PRINCE, D. A. Sodium channels in dendrites of rat cortical pyramidal neurons. *Proc. Natl. Acad. Sci. USA* 86: 2473–2477, 1989.

HUGUENARD, J. R. AND PRINCE, D. A. Slow inactivation of a TEA-sensitive K current in acutely isolated rat thalamic relay neurons. *J. Neurophysiol.* 66: 1316–1328, 1991.

HUGUENARD, J. R. AND PRINCE, D. A. A novel T-type current with slowed inactivation contributes to prolonged Ca^{2+}-dependent burst firing in GABAergic neurons of rat thalamic reticular nucleus. *J. Neurosci.* In press.

JAHNSEN, H. AND LLINÁS, R. R. Electrophysiological properties of guinea-pig thalamic neurons: an in vitro study. *J. Physiol. Lond.* 349: 205–226, 1984a.

JAHNSEN, H. AND LLINÁS, R. R. Ionic basis for the electroresponsiveness and oscillatory properties of guinea-pig thalamic neurons in vitro. *J. Physiol. Lond.* 349: 227–247, 1984b.

LLINÁS, R. AND JAHNSEN, H. Electrophysiology of mammalian thalamic neurons in vitro. *Nature Lond.* 297: 406–408, 1982.

MASTRONARDE, D. N. Two classes of single-input X-cells in cat lateral geniculate nucleus. II. Retinal inputs and the generation of receptive-field properties. *J. Neurophysiol.* 57: 381–413, 1987.

MCCORMICK, D. A. Functional properties of a slowly inactivating potassium current in guinea pig dorsal lateral geniculate relay neurons. *J. Neurophysiol.* 66: 1176–1189, 1991.

MCCORMICK, D. A. AND FEESER, H. R. Functional implications of burst firing and single spike activity in lateral geniculate relay neurons. *Neuroscience* 39: 103–113, 1990.

MCCORMICK, D. A. AND HUGUENARD, J. R. A model of the electrophysiological properties of thalamocortical relay neurons. *J. Neurophysiol.* 68: 1384–1400, 1992.

MCCORMICK, D. A. AND PAPE, H.-C. Properties of a hyperpolarization-activated cation current and its role in rhythmic oscillation in thalamic relay neurons. *J. Physiol. Lond.* 431: 291–318, 1990.

MCCORMICK, D. A. AND PRINCE, D. A. Noradrenergic modulation of firing pattern in guinea pig and cat thalamic neurons, in vitro. *J. Neurophysiol.* 59: 978–996, 1988.

NOBEL, D., DIFRANCESCO, D., AND DENYER, J. Ionic mechanisms in normal and abnormal cardiac pacemaker activity. In: *Neuronal and Cellular Oscillators,* edited by J. W. Jacklet. New York: Dekker, 1989, p. 59–85.

PAPE, H.-C. AND MCCORMICK, D. A. Noradrenalin and serotonin selectively modulate thalamic burst firing by enhancing a hyperpolarization-activated cation current. *Nature Lond.* 340: 715–718, 1989.

REGAN, L. J. Voltage-dependent calcium currents in purkinje cells from rat cerebellar vermis. *J. Neurosci.* 11: 2259–2269, 1991.

SHOSAKU, A., KAYAMA, Y., SUMITOMO, I., SUGITANI, M., AND IWAMA, K. Analysis of recurrent inhibitory circuit in rat thalamus: neurophysiology of the thalamic reticular nucleus. *Prog. Neurobiol.* 32: 77–102, 1989.

SOLTESZ, I., LIGHTOWLER, S., LERESCHE, N., JASSIK-GERSCHENFELD, D., POLLARD, C. E., AND CRUNELLI, V. Two inward currents and the transformation of low frequency oscillations of rat and cat thalamocortical cells. *J. Physiol. Lond.* 441: 175–197, 1991.

STERIADE, M., CURRO DOSSI, R., AND NUNEZ, A. Network modulation of a slow intrinsic oscillation of cat thalamocortical neurons implicated in sleep delta waves: cortically induced synchronization and brainstem cholinergic suppression. *J. Neurosci.* 11: 3200–3217, 1991.

STERIADE, M. AND DESCHÊNES, M. The thalamus as a neuronal oscillator. *Brain Res. Rev.* 8: 1–63, 1984.

STERIADE, M. AND LLINÁS, R. R. The functional states of the thalamus and the associated neuronal interplay. *Physiol. Rev.* 68: 649–742, 1988.

STORM, J. F. Potassium currents in hippocampal cells. *Prog. Brain Res.* 83: 161–187, 1990.

SUZUKI, S. AND ROGAWSKI, M. A. T-type calcium channels mediate the transition between tonic and phasic firing in thalamic neurons. *Proc. Natl. Acad. Sci. USA* 86: 7228–7233, 1989.

WANG, X.-J., RINZEL, J., AND ROGAWSKI, M. A. A model of the T-type calcium current and the low-threshold spike in thalamic neurons. *J. Neurophysiol.* 66: 839–850, 1991.